Structural Engineering and Mechanics, Vol. 38, No. 6 (2011) 733-751
DOI: http://dx.doi.org/10.12989/sem.2011.38.6.733

The construction of multivariable Reissner-Mindlin plate elements based on B-spline wavelet on the interval

Xingwu Zhang, Xuefeng Chen* and Zhengjia He

State Key Laboratory for Manufacturing System Engineering, School of Mechanical Engineering, Xi'an Jiaotong University, Xi'an 710049, PR China

(Received May 6, 2010, Accepted February 22, 2011)

Abstract. In the present study, a new kind of multivariable Reissner-Mindlin plate elements with two kinds of variables based on B-spline wavelet on the interval (BSWI) is constructed to solve the static and vibration problems of a square Reissner-Mindlin plate, a skew Reissner-Mindlin plate, and a Reissner-Mindlin plate on an elastic foundation. Based on generalized variational principle, finite element formulations are derived from generalized potential energy functional. The two-dimensional tensor product BSWI is employed to form the shape functions and construct multivariable BSWI elements. The multivariable wavelet finite element method proposed here can improve the solving accuracy apparently because generalized stress and strain are interpolated separately. In addition, compared with commonly used Daubechies wavelet finite element method, BSWI has explicit expression and a very good approximation property which guarantee the satisfying results. The efficiency of the proposed multivariable Reissner-Mindlin plate elements are verified through some numerical examples in the end.

Keywords: multivariable; B-spline wavelet on the interval; Reissner-Mindlin plate; static analysis; vibration analysis

1. Introduction

Ressiner-Mindlin plate is a widely used structure in engineering and many scholars have done much research on it. A lot of finite elements have been constructed to do static and vibration analysis (Zienkiewicz *et al.* 2005, Brezzi *et al.* 1989, Bathe *et al.* 1990, Lee and Bathe 2010, Long *et al.* 2004, Xiang *et al.* 2010, Hu *et al.* 2010, Liu *et al.* 2009, Liu and Soh 2007) and yielded satisfactory results. Liu *et al.* (2009) constructed a Mindlin pseudospectral plate element to perform static, dynamic, and wave propagation analysis of plate-like structures. Lee and Bathe (2010) constructed MITC plate and MITC shell elements and verified their efficiency. In Monograph (Zienkiewicz *et al.* 2005), Zienkiewicz *et al.* (2005) presented the fundamentals for structural analysis and constructed many classical elements.

In the above elements, they mainly takes the traditional interpolating function to discrete the solving field. Wavelet finite element method is a new numerical method that uses scaling and

*Corresponding author, Professor, E-mail: chenxf@mail.xjtu.edu.cn

wavelet functions to substitute polynomials used in conventional method. Based on the good properties such as multiresolution and orthogonality of the wavelet, wavelet finite element method is superior to other traditional methods, and is the subject of much research in numerical calculation (Canuto *et al.* 1996, 2000, Cohen 2003, Steffen *et al.* 2009) and structural analysis (Chen and Wu 1996, Chen *et al.* 2004, Wang *et al.* 2010, Xiang *et al.* 2007, He and Chen 2008, Han *et al.* 2005, Diaz *et al.* 2009). By comparing numerical methods in engineering numerical calculations, Basu (2003) pointed out that the wavelet method could possibly replace the finite element, boundary element, and element-free methods in the near future.

The multivariable finite element method is based on the generalized potential energy functional (Hellinger 1914, Reissner 1950, Hu 1954, Washizu 1955), which separately calculates generalized stress and strain to avoid the integration and differentiation of generalized displacement, and improve their accuracy. Shen and He (1995), Shen *et al.* (1992) conducted many studies on the multivariable finite element method. Using the spline function as the trial function, he constructed many elements such as beam, plate, shell, and so on, proving the advantages of multivariable finite element method in the calculation of generalized stress and strain. However, the spline function has its limitations. For example, it does not have the properties such as localization, multiresolution, orthogonality and so on.

Multivariable wavelet finite element method makes full use of the advantages of combining wavelet and multivariable finite element together. Han *et al.* (2005) constructed the multivariable wavelet finite element of a Reissner-Mindlin plate and analyzed the bending problem. He used interpolating wavelet as trial function and obtained satisfactory results. However, interpolating wavelets do not have explicit expression, which makes the calculation of integration and differentiation difficult.

In this paper, a new multivariable BSWI element with two kinds of variables (TBSWI) for a Reissner-Mindlin plate is constructed. BSWI has explicit expression, which makes integration and differentiation convenient. Furthermore, it has the best approximation of numerical calculation among all existing wavelets (Cohen 2003). The bending and vibration problems of a square Reissner-Mindlin plate, a skew Reissner-Mindlin plate, and a Reissner-Mindlin plate on an elastic foundation are analyzed, and several numerical examples are provided. The efficiency and veracity of the results are verified by comparing them with those in the studies of Han *et al.* (2005), Xiang and Chen (2006) and Long and Xi (1992).

2. Two-dimensional tensor product BSWI on the interval [0,1]

The B-spline functions for a given simple knot sequence can be constructed by taking the piecewise polynomials between the knots and joining them together at the knots to obtain a certain order of overall smoothness. Chui and Quak constructed BSWI (Chui and Quak 1992), and presented its decomposition and reconstruction algorithm in 1994 (Quak and Weyrich 1994). Therefore, we can obtain the one-dimensional multiresolution analysis of BSWI on the interval [0,1] and the scaling function ϕ and corresponding wavelets ψ in the multiresolution approximation space V_j. According to the 0 scale mth order B-spline functions and the corresponding wavelets given by Goswami *et al.* (1995), the j scale mth order BSWI (BSWImj) scaling functions $\phi_{m,k}^{j}(\xi)$ and the corresponding wavelets $\psi_{m,k}^{j}(\xi)$ can be evaluated by the following formulas

$$\phi_{m,k}^{j}(\xi)=\begin{cases}\phi_{m,k}^{l}(2^{j-l}\xi),\ k=-m+1,\ldots,-1 & \text{(0 boundary scaling functions)}\\ \phi_{m,2^{j}-m-k}^{l}(1-2^{j-l}\xi),\ k=2^{j}-m+1,\ldots,2^{l}-1 & \text{(1 boundary scaling functions)}\\ \phi_{m,0}^{l}(2^{j-l}\xi-2^{-l}k),\ k=0,\ldots,2^{j}-m & \text{(inner scaling functions)}\end{cases} \tag{1}$$

$$\psi_{m,k}^{j}(\xi)=\begin{cases}\psi_{m,k}^{l}(2^{j-l}\xi),\ k=-m+1,\ldots,-1 & \text{(0 boundary wavelets)}\\ \psi_{m,2^{j}-2m-k+1}^{l}(1-2^{j-l}\xi),\ k=2^{j}-2m+2,\ldots,2^{l}-m & \text{(1 boundary wavelets)}\\ \psi_{m,0}^{l}(2^{j-l}\xi-2^{-l}k),\ k=0,\ldots,2^{j}-2m+1 & \text{(inner wavelets)}\end{cases} \tag{2}$$

Thus, the scaling function on the interval [0,1] can be obtained in vector form as follows

$$\boldsymbol{\phi}=\{\phi_{m,-m+1}^{j}(\xi)\ \ \phi_{m,-m+2}^{j}(\xi)\ \ldots\ \phi_{m,2^{j}-1}^{j}(\xi)\} \tag{3}$$

where, $\phi_{m,-m+1}^{j}(\xi)\ \ \phi_{m,-m+2}^{j}(\xi)\ \ldots\ \phi_{m,2^{j}-1}^{j}(\xi)$ are the scaling functions obtained from Eq. (1).

The vector form of wavelets is

$$\boldsymbol{\Psi}=\{\psi_{m,-m+1}^{j}(\xi)\ \ \psi_{m,-m+2}^{j}(\xi)\ \ldots\ \psi_{m,2^{j}-m}^{j}(\xi)\} \tag{4}$$

where, $\psi_{m,-m+1}^{j}(\xi)\ \ \psi_{m,-m+2}^{j}(\xi)\ \ldots\ \psi_{m,2^{j}-m}^{j}(\xi)$ are the wavelets obtained by Eq. (2).

Through the tensor product, the two-dimensional BSWI at scale j in $L^{2}(R^{2})$ can be generated by multiresolution approximation space V_{j}^{1} and V_{j}^{2}. The tensor product space $F_{j}=V_{j}^{1}\otimes V_{j}^{2}$.

The two-dimensional scaling functions are

$$\boldsymbol{\Phi}=\boldsymbol{\phi}_{1}\otimes\boldsymbol{\phi}_{2} \tag{5}$$

where $\boldsymbol{\phi}_{1}=\{\phi_{m,-m+1}^{j}(\xi)\ \ \phi_{m,-m+2}^{j}(\xi)\ \ldots\ \phi_{m,2^{j}-1}^{j}(\xi)\}$ is the one row vector combined by the scaling functions for m at the scale j and $\boldsymbol{\phi}_{2}=\{\phi_{m,-m+1}^{j}(\eta)\ \ \phi_{m,-m+2}^{j}(\eta)\ \ldots\ \phi_{m,2^{j}-1}^{j}(\eta)\}$ is the other row vector combined by the scaling functions for m at the scale j. $\otimes$ is the kronecker symbol.

While the two-dimensional wavelet functions are

$$\boldsymbol{\psi}^{1}=\boldsymbol{\phi}_{1}\otimes\boldsymbol{\psi}_{2} \tag{6}$$

$$\boldsymbol{\psi}^{2}=\boldsymbol{\psi}_{1}\otimes\boldsymbol{\phi}_{2} \tag{7}$$

$$\boldsymbol{\psi}^{3}=\boldsymbol{\psi}_{1}\otimes\boldsymbol{\psi}_{2} \tag{8}$$

where, $\boldsymbol{\phi}_{1}$ and $\boldsymbol{\phi}_{2}$ are the vector form of scaling functions in Eq. (3) and $\boldsymbol{\psi}_{1}$ and $\boldsymbol{\psi}_{2}$ are wavelets of BSWI*mj* in Eq. (4).

Fig. 1(a) shows all the scaling functions $\boldsymbol{\Phi}$ of the two-dimensional tensor products BSWI. Fig. 1(b) is the figure of all tensor product BSWI wavelets $\boldsymbol{\psi}^{1}$. Figs. 1(c) and (d) show other two tensor product wavelets $\boldsymbol{\psi}^{2}$ and $\boldsymbol{\psi}^{3}$. They are generated by $BSWI4_{3}$, and the expressions of $BSWI4_{3}$ can be found in Zhang *et al.* (2010).

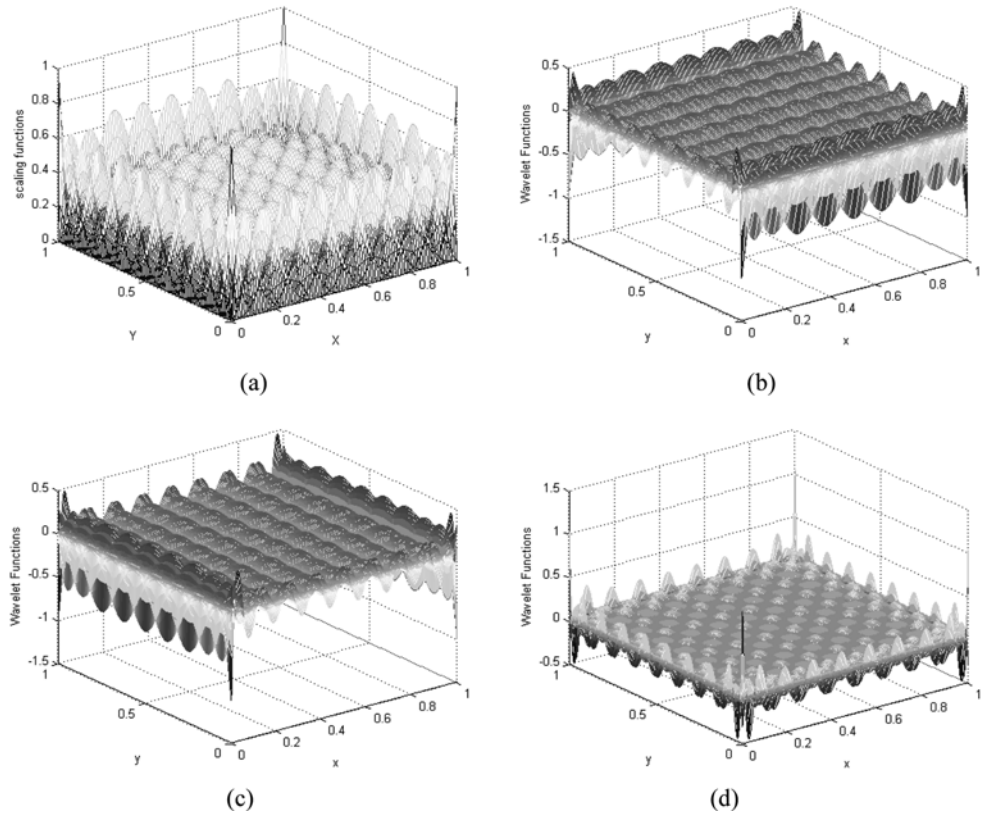

Fig. 1 Two-dimensional tensor product BSWI; (a) scaling functions $\Phi = \phi_1 \otimes \phi_2$ and (b) wavelets $\psi^1 = \phi_1 \otimes \psi_2$, (c) wavelets $\psi^2 = \psi_1 \otimes \phi_2$ and (d) wavelets $\psi^3 = \psi_1 \otimes \psi_2$

3. The construction of TBSWI element for square and skew Reissner-Mindlin plate

3.1 TBSWI element formulation for static and vibration analysis of square and skew Reissner-Mindlin plate

Fig. 2 shows that the skew coordinate is necessary to analyze the static and vibration problems for square and skew Reissner-Mindlin plates. The relationship between skew coordinate xoy and rectangular coordinate $\bar{x}\bar{o}\bar{y}$ is as follows (Shen 1991)

$$\begin{bmatrix} \bar{x} \\ \bar{y} \end{bmatrix} = \begin{bmatrix} 1 & \cos\alpha \\ 0 & \sin\alpha \end{bmatrix} \begin{bmatrix} x \\ y \end{bmatrix} \tag{9}$$

$$\begin{bmatrix} x \\ y \end{bmatrix} = \begin{bmatrix} 1 & -1/\tan\alpha \\ 0 & 1/\sin\alpha \end{bmatrix} \begin{bmatrix} \bar{x} \\ \bar{y} \end{bmatrix} \tag{10}$$

Under homogeneous boundary conditions, the generalized potential energy function with two kinds of variables for bending and vibration problems of Reissner-Mindlin plate in rectangular

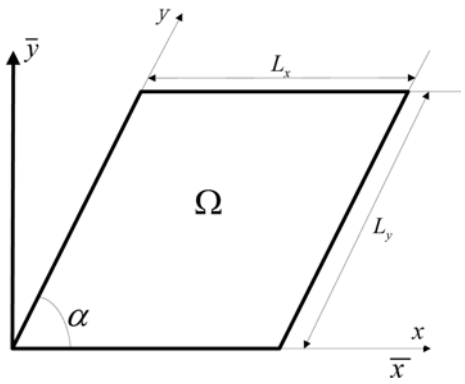

Fig. 2 The solving domain and relative parameters of Reissner-Mindlin plate

coordinate is (Shen 1997)

$$\Pi_{2p} = \int_{\Omega} \mathbf{M}^T \chi d\bar{x}d\bar{y} + \int_{\Omega} \mathbf{Q}^T \gamma d\bar{x}d\bar{y} - \int_{\Omega} \frac{1}{2} \mathbf{M}^T \mathbf{D}_b^{-1} \mathbf{M} d\bar{x}d\bar{y} - \int_{\Omega} \frac{1}{2} \mathbf{Q}^T C_b^{-1} \mathbf{Q} d\bar{x}d\bar{y}$$
$$- \int_{\Omega} \Delta^T \mathbf{P} d\bar{x}d\bar{y} - \frac{1}{2} \int_{\Omega} \omega^2 \bar{m} w^2 d\bar{x}d\bar{y} \tag{11}$$

The symbols Δ and **M**, **Q** are independent functions namely displacement field function, internal moment field function, and shear field function, respectively. Accordingly, there are eight degrees of freedom (DOFs) in every node.

$$\Delta = [w \quad \theta_x \quad \theta_y]^T$$

$$\mathbf{M} = [M_x \quad M_y \quad M_{xy}]^T$$

$$\mathbf{Q} = [Q_x \quad Q_y]^T$$

where

$\bar{m}$ is the area density

ω is the vibration eigen values

P is the load matrix

$\mathbf{P} = [q \quad 0 \quad 0]^T$

$\chi = -\mathbf{D}_1^T \Delta$

$\gamma = \mathbf{E}_1^T \Delta$

$\mathbf{D}_1$ and $\mathbf{E}_1$ are the matrix differential operators.

$$\mathbf{D}_1 = \begin{bmatrix} 0 & 0 & 0 \\ \frac{\partial}{\partial \bar{x}} & 0 & \frac{\partial}{\partial \bar{y}} \\ 0 & \frac{\partial}{\partial \bar{y}} & \frac{\partial}{\partial \bar{x}} \end{bmatrix}$$

$$\mathbf{E}_1 = \begin{bmatrix} \dfrac{\partial}{\partial \bar{x}} & \dfrac{\partial}{\partial \bar{y}} \\ -1 & 0 \\ 0 & -1 \end{bmatrix}$$

According to Eq. (9), we have the following sub-equations

$$\chi = \left\{ -\frac{\partial \theta_{\bar{x}}}{\partial \bar{x}} \quad -\frac{\partial \theta_{\bar{y}}}{\partial \bar{y}} \quad -\left(\frac{\partial \theta_{\bar{x}}}{\partial \bar{y}} + \frac{\partial \theta_{\bar{y}}}{\partial \bar{x}} \right) \right\}^T$$

$$= \left\{ -\frac{\partial \theta_x}{\partial x} \quad \left(\frac{\cos\alpha}{\sin\alpha} \frac{\partial \theta_y}{\partial x} - \frac{1}{\sin\alpha} \frac{\partial \theta_y}{\partial y} \right) \quad -\left(-\frac{\cos\alpha}{\sin\alpha} \frac{\partial \theta_x}{\partial x} + \frac{1}{\sin\alpha} \frac{\partial \theta_x}{\partial y} + \frac{\partial \theta_y}{\partial x} \right) \right\} \tag{12}$$

$$\gamma = -\left\{ \frac{\partial w}{\partial \bar{x}} - \theta_{\bar{x}} \quad \frac{\partial w}{\partial \bar{y}} - \theta_{\bar{y}} \right\}^T$$

$$= -\left\{ \frac{\partial w}{\partial x} - \theta_x \quad -\frac{\cos\alpha}{\sin\alpha} \frac{\partial w}{\partial x} - \frac{1}{\sin\alpha} \frac{\partial w}{\partial y} - \theta_y \right\} \tag{13}$$

$\mathbf{D}_b$ is the elastic matrix

$$\mathbf{D}_b = D_0 \begin{bmatrix} 1 & \mu & 0 \\ \mu & 1 & 0 \\ 0 & 0 & \dfrac{1-\mu}{2} \end{bmatrix} \tag{14}$$

where

μ is Poisson ratio

D_0 is bending rigidity

$$D_0 = \frac{Et^3}{12(1-\mu^2)} \tag{15}$$

where

E is elastic modulus

t is thickness of the plate

$$C_b = \frac{5Et}{12(1+\mu)} \tag{16}$$

As shown in Fig. 2, the coordinate values are: $x \in [0, L_x]$, $y \in [0, L_y]$. We define transformation formula $\xi = x/L_x$ $(0 \le \xi \le 1)$, $\eta = y/L_y$ $(0 \le \eta \le 1)$, so the coordinate (x, y) can be mapped into standard solving domain [0,1] × [0,1].

By using the scaling functions of the two-dimensional tensor product BSWI $\Phi = \phi_1 \otimes \phi_2$ in Eq. (5) as the interpolating function and translating all the field variables into standard solving domain, the displacement field function can be obtained as follows

$$\Delta(\xi,\eta)=\begin{bmatrix} w \\ \theta_\xi \\ \theta_\eta \end{bmatrix}=\begin{bmatrix} \mathbf{\Phi T}^e & 0 & 0 \\ 0 & \mathbf{\Phi T}^e & 0 \\ 0 & 0 & \mathbf{\Phi T}^e \end{bmatrix}\begin{bmatrix} w^e \\ \theta_\xi^e \\ \theta_\eta^e \end{bmatrix} \tag{17}$$

The internal moment field function is as follows

$$\mathbf{M}(\xi,\eta)=\begin{bmatrix} M_\xi \\ M_\eta \\ M_{\xi\eta} \end{bmatrix}=\begin{bmatrix} \mathbf{\Phi T}^e & 0 & 0 \\ 0 & \mathbf{\Phi T}^e & 0 \\ 0 & 0 & \mathbf{\Phi T}^e \end{bmatrix}\begin{bmatrix} M_\xi^e \\ M_\eta^e \\ M_{\xi\eta}^e \end{bmatrix} \tag{18}$$

The shear field function is as follows

$$\mathbf{Q}(\xi,\eta)=\begin{bmatrix} Q_\xi \\ Q_\eta \end{bmatrix}=\begin{bmatrix} \mathbf{\Phi T}^e & 0 \\ 0 & \mathbf{\Phi T}^e \end{bmatrix}\begin{bmatrix} Q_\xi^e \\ Q_\eta^e \end{bmatrix} \tag{19}$$

where $\mathbf{\Phi}$ is the two-dimensional scaling functions in Eq. (5) and $\mathbf{T}^e$ is the transformation matrix. The details can be seen in Xiang and Chen (2006).

Taking Eqs. (12)-(19) and transformation formula (9) into Eq. (11), according to the generalized variational principle $\delta\Pi_{2p}/\partial M_\xi^e=0, \delta\Pi_{2p}/\partial M_\eta^e=0, \delta\Pi_{2p}/\partial M_{\xi\eta}^e=0, \delta\Pi_{2p}/\partial Q_\xi^e=0$, $\delta\Pi_{2p}/\partial Q_\eta^e=0$, $\delta\Pi_{2p}/\partial\theta_\xi^e=0$, $\delta\Pi_{2p}/\partial\theta_\eta^e=0$, and $\delta\Pi_{2p}/\partial w^e=0$, we can obtain the TBSWI element formulation for bending and vibration problems of square and skew Reissner-Mindlin plates as follows

$$\begin{bmatrix} \mathbf{F} & \mathbf{H} \\ \mathbf{H}^T & 0 \end{bmatrix}\begin{bmatrix} \mathbf{a} \\ \mathbf{b} \end{bmatrix}=\begin{bmatrix} 0 \\ \mathbf{p} \end{bmatrix}+\begin{bmatrix} 0 \\ \mathbf{M}_\lambda \end{bmatrix} \tag{20}$$

where

$$\mathbf{F}=\begin{bmatrix} \frac{-12}{Et^3}\sin\alpha\Gamma_1^{00}\otimes\Gamma_2^{00} & \frac{12\mu}{Et^3}\sin\alpha\Gamma_1^{00}\otimes\Gamma_2^{00} & 0 & 0 & 0 \\ \frac{12\mu}{Et^3}\sin\alpha\Gamma_1^{00}\otimes\Gamma_2^{00} & \frac{-12}{Et^3}\sin\alpha\Gamma_1^{00}\otimes\Gamma_2^{00} & 0 & 0 & 0 \\ 0 & 0 & \frac{-24(1+\mu)}{Et^3}\sin\alpha\Gamma_1^{00}\otimes\Gamma_2^{00} & 0 & 0 \\ 0 & 0 & 0 & \frac{-12(1+\mu)}{5Et}\sin\alpha\Gamma_1^{00}\otimes\Gamma_2^{00} & 0 \\ 0 & 0 & 0 & 0 & \frac{-12(1+\mu)}{5Et}\sin\alpha\Gamma_1^{00}\otimes\Gamma_2^{00} \end{bmatrix}$$

$$\mathbf{H}=\begin{bmatrix} 0 & -\sin\alpha\Gamma_1^{01}\otimes\Gamma_2^{00} & 0 \\ 0 & 0 & \cos\alpha\Gamma_1^{01}\otimes\Gamma_2^{00}-\Gamma_1^{00}\otimes\Gamma_2^{01} \\ 0 & \cos\alpha\Gamma_1^{01}\otimes\Gamma_2^{00}-\Gamma_1^{00}\otimes\Gamma_2^{01} & -\sin\alpha\Gamma_1^{01}\otimes\Gamma_2^{00} \\ -\sin\alpha\Gamma_1^{01}\otimes\Gamma_2^{00} & \sin\alpha\Gamma_1^{00}\otimes\Gamma_2^{00} & 0 \\ \cos\alpha\Gamma_1^{01}\otimes\Gamma_2^{00}-\Gamma_1^{00}\otimes\Gamma_2^{01} & 0 & \sin\alpha\Gamma_1^{00}\otimes\Gamma_2^{00} \end{bmatrix}$$

$$\mathbf{a} = [M_\xi^e \;\; M_\eta^e \;\; M_{\xi\eta}^e \;\; Q_\xi^e \;\; Q_\eta^e]^T$$

$$\mathbf{b} = [w^e \;\; \theta_\xi^e \;\; \theta_\eta^e]^T$$

$$\mathbf{M}_\lambda = \overline{m}\Gamma_1^{00} \otimes \Gamma_2^{00} w^e$$

To distributed load, $\mathbf{P} = [(\mathbf{T}^e)^T L_x L_y \sin\alpha \int_0^1 \int_0^1 q\boldsymbol{\phi}_1^T \otimes \boldsymbol{\phi}_2^T d\xi d\eta \;\; 0 \;\; 0]^T$. To concentrated load, $\mathbf{P} = [(\mathbf{T}^e)^T L_x L_y \sin\alpha \int_0^1 \int_0^1 q\,\delta(\xi - \xi_1)\delta(\eta - \eta_1)\boldsymbol{\phi}_1^T \otimes \boldsymbol{\phi}_2^T d\xi d\eta \;\; 0 \;\; 0]^T$, where ξ_1 and η_1 are the coordinates at the concentrated load point.

Therefore, the formulation for plate bending analysis is as follows

$$\begin{bmatrix} \mathbf{F} & \mathbf{H} \\ \mathbf{H}^T & 0 \end{bmatrix} \begin{bmatrix} \mathbf{a} \\ \mathbf{b} \end{bmatrix} = \begin{bmatrix} 0 \\ \mathbf{P} \end{bmatrix} \tag{21}$$

The formulation for vibration analysis is

$$\begin{bmatrix} \mathbf{F} & \mathbf{H} \\ \mathbf{H}^T & 0 \end{bmatrix} \begin{bmatrix} \mathbf{a} \\ \mathbf{b} \end{bmatrix} = \begin{bmatrix} 0 \\ \mathbf{M}_\lambda \end{bmatrix} \tag{22}$$

The frequency equation to free vibration is as follows

$$\left| \mathbf{K} - \omega^2 \mathbf{M}_\lambda \right| = 0 \tag{23}$$

where

$$\mathbf{K} = \begin{bmatrix} \mathbf{F} & \mathbf{H} \\ \mathbf{H}^T & 0 \end{bmatrix}$$

The integral terms are as follows

$$\Gamma_1^{00} = (\mathbf{T}^e)^T L_x \int_0^1 \boldsymbol{\Phi}_1^T \boldsymbol{\Phi}_1 d\xi (\mathbf{T}^e)$$

$$\Gamma_1^{10} = (\mathbf{T}^e)^T \int_0^1 \frac{d\boldsymbol{\Phi}_1^T}{d\xi} \boldsymbol{\Phi}_1 d\xi (\mathbf{T}^e)$$

$$\Gamma_1^{20} = (\mathbf{T}^e)^T \frac{1}{L_x} \int_0^1 \frac{d^2\boldsymbol{\Phi}_1^T}{d\xi^2} \boldsymbol{\Phi}_1 d\xi (\mathbf{T}^e)$$

$$\Gamma_1^{01} = (\Gamma_1^{10})^T$$

$$\Gamma_1^{02} = (\Gamma_1^{20})^T$$

We can obtain $\Gamma_1^{i,j}(i,j = 0, 1, 2)$ by substituting L_x and $d\xi$ with L_y and $d\eta$ in $\Gamma_2^{i,j}(i,j = 0, 1, 2)$.

Following Eqs. (21), (22), and (23), we can conduct a static and vibration analysis of square and skew Reissner-Mindlin plates with two kinds of variables, similar to the traditional finite element method.

3.2 Numerical examples

In order to verify the TBSWI element for square and skew Reissner-Mindlin plate, several numerical examples of the bending and vibration analysis for Reissner-Mindlin plates are provided here. $BSWI4_3$ (the 4^{th} order BSWI scaling functions at scale $j = 3$) in Fig. 1(a) is chosen as the interpolating function.

Fig. 3 shows the nodes displacement, solving domain and the displacement of interpolating functions. The solving domain is divided into one TBSWI element, and interpolated by two-dimensional tensor product BSWI. The relative parameters are as follows: length $L = L_x = L_y = 1$ m; Elastic modulus $E = 3\times10^4$ N/m^2; Poisson ratio $\mu = 0.3$; Aera density $\overline{m} = 7917$ kg/m^3; Uniform load $q = -1$ N/m^2; Concentrated load $q = -1$ N.

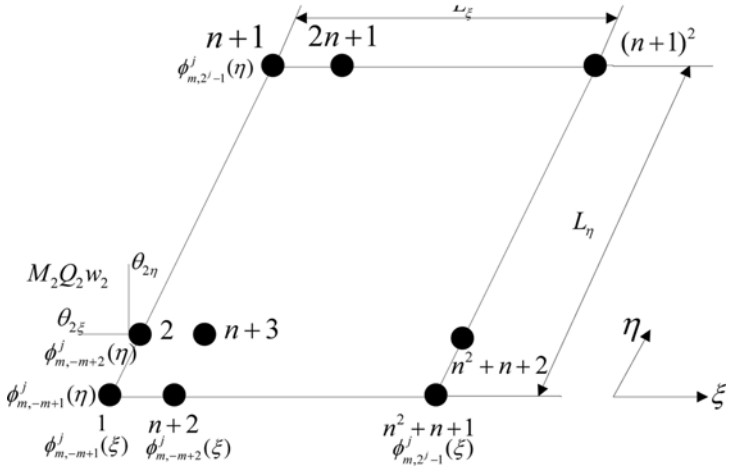

Fig. 3 The solving domain, node placement and the displacement of interpolating functions

Table 1 Central displacement of a square Reissner-Mindlin plate with distributed load under different boundary conditions

t/L	$100wD_0/qL^4$ (simply supported)				$100wD_0/qL^4$ (clamp supported)			
	TBSWI	Long	Han	Theoretical	TBSWI	Long	Han	Theoretical
	968DOFs	1200DOFs	968DOFs	/	968DOFs	1200DOFs	968DOFs	/
0.01	0.4064	0.4045	/	0.4062	0.1268	0.1293	/	0.1265
0.1	0.4273	0.4242	0.4269	0.4273	0.1505	0.1521	0.1493	0.1499
0.2	0.4904	0.4869	0.4887	0.4906	0.2172	0.2181	0.2166	0.2167
0.3	0.5957	0.5902	0.5952	0.5956	0.3246	0.3229	0.3224	0.3227
0.35	0.6641	0.6564	0.6631	0.6641	0.3937	0.3896	0.3948	0.3951

Table 2 Displacement and moment of a square Reissner-Mindlin plate under distributed load

t/L	Method	DOFs	$100wD_0/qL^4$ (displacement)		$M//qL^2$ (moment)	
			Simply supported	Clamp supported	Simply supported (midpoint)	Clamp supported (midpoint of boundary)
0.001	TBSWI	968	0.4062	0.1265	0.0479	-0.0514
	Long	1200	0.4043	0.1293	0.0480	-0.0506
	Theoretical solution	/	0.4062	0.1265	0.0479	-0.0513
0.3	TBSWI	968	0.5957	0.3246	0.0479	-0.0444
	Long	1200	0.5902	0.3229	0.0489	-0.0458
	Han	968	0.5953	0.3226	0.0481	-0.0418
	Theoretical solution	/	0.5956	0.3227	0.0479	-0.0426

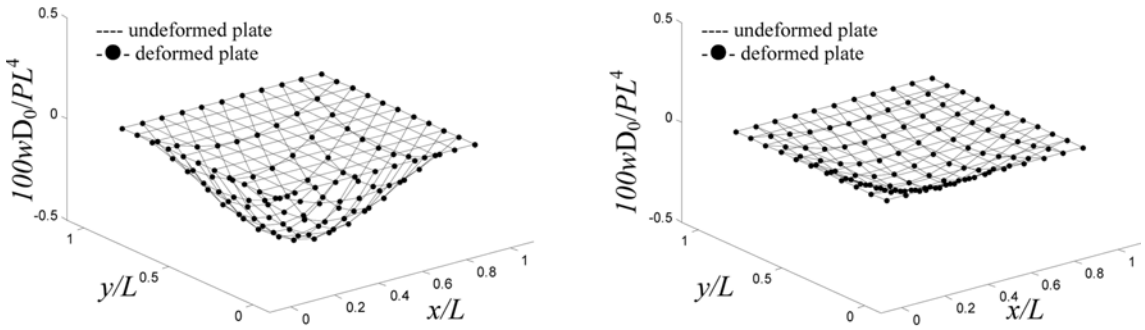

Fig. 4 The deformation map of a Reissner-Mindlin plate with $t/L = 0.2$

Tables 1 and 2 are two examples of square Reissner-Mindlin plate bending. The central displacement and moment of simply and clamp supported Reissner-Mindlin plates are calculated. From the table data, we can see that the results of this study agree with those in exact solution. Besides, a comparison with the methods in references (Long and Xi 1992, Han *et al.* 2005) indicates that TBSWI element is superior, and that the results here are better than those in the references. The deformation map in Fig. 4 shows the overall deformation trend which indicates the entire results here in consistent to the practical situations.

In Tables 3 and 4, the vibration problems of the square Reissner-Mindlin plates are analyzed under two different boundary conditions. To six different thick/long ratio, the table data show that the results of TBSWI element agree with spline FEM in reference (Shen 1991). Furthermore, to thin plate results, the TBSWI results are very close to the exact value of thin plate in references (Warburton 1954, Hu 1981), it proves that TBSWI element can avoid the shear locking problem. That is, TBSWI element is not only efficient in the bending and vibration analysis of Reissner-Mindlin plate, but also suitable for thin plate.

Table 3 The first five natural frequencies of a simply supported square Reissner-Mindlin plate (Frequency parameters $\Omega_i = \omega_i L^2(\rho t/D_0)^{1/2}(\mathrm{rad}\cdot\mathrm{s}^{-1})$)

t/L	Methods	DOFs	Ω_1	Ω_2	Ω_3	Ω_4	Ω_5
0.001	TBSWI	968	19.73915	49.34760	49.34760	78.95580	98.68783
0.01	TBSWI	968	19.73364	49.31320	49.31320	78.86778	98.55038
	Spline FEM	2904	19.54310	49.34299	49.36815	78.91379	101.15355
0.02	TBSWI	968	19.71698	49.20938	49.20938	78.60285	98.13734
	Spline FEM	2904	19.60819	49.06273	49.07697	78.23098	98.59930
0.05	TBSWI	968	19.60151	48.50057	48.50057	76.82017	98.38453
	Spline FEM	2904	19.21942	47.73099	47.76030	74.98730	94.11515
0.1	TBSWI	968	19.20507	46.19845	46.19845	71.32081	87.16275
	Spline FEM	2904	18.31740	44.34606	44.51496	67.42929	84.06901
0.2	TBSWI	968	17.83023	39.45972	39.45972	57.24563	67.65447
	Spline FEM	2904	16.04482	36.15783	37.00329	52.13606	63.767
Exact of thin plate		/	19.74	49.35	49.35	78.95	98.64

Table 4 The first five natural frequencies of a clamp supported square Reissner-Mindlin plate (Frequency parameters $\Omega_i = \omega_i L^2(\rho t/D_0)^{1/2}(\mathrm{rad}\cdot\mathrm{s}^{-1})$)

t/L	Methods	DOFs	Ω_1	Ω_2	Ω_3	Ω_4	Ω_5
0.001	TBSWI	968	35.98506	73.39294	73.39294	108.21912	131.54766
0.01	TBSWI	968	35.94667	73.25806	73.25806	107.94153	131.16350
	Spline FEM	2904	35.95932	73.92233	73.93530	108.76511	139.23087
0.02	TBSWI	968	35.83142	72.85473	72.85473	107.11670	130.20960
	Spline FEM	2904	35.81282	72.95158	72.95242	107.15167	132.09457
0.05	TBSWI	968	35.06501	70.23374	70.23374	101.92805	122.82260
	Spline FEM	2904	34.96382	69.84711	69.84833	101.00397	122.01418
0.1	TBSWI	968	32.75858	62.92107	62.92107	88.63382	104.64989
	Spline FEM	2904	32.42808	61.83785	61.83844	86.37923	102.14913
0.2	TBSWI	968	26.89462	47.41137	47.41137	63.93589	73.12864
	Spline FEM	2904	26.31114	45.92644	45.92652	61.28589	70.22099
Exact of thin plate		/	35.98800	73.73657	/	108.16	132.25

Tables 5 and 6 show the bending analysis of skew Reissner-Mindlin plate under different boundary conditions and skew angles. The results of TBSWI element are compared with SHELL63 and other elements in references (Xiang *et al.* 2007, Rao and Chaudhary 1998, Morley 1963). Skew angle α is chosen from 30 to 90 degree. The TBSWI solutions match well with those of the other methods. The comparison with SHELL63 indicates that TBSWI (968DOFs) can obtain solution in same accuracy of SHELL63 (38400DOFs) with much smaller DOFs, only 2.6% DOFs of SHELL63 element, which proves the superiority of TBSWI element. Besides, especially to moment, TBSWI can obtain results with great accuracy than BSWI element. Furthermore, by comparison with 'exact

Table 5 Central displacement and moment of a skew Reissner-Mindlin plate under distributed load

Skew angle α	$w1000D_0/qL^4$ (simply supported)					$M10/qL^2$ (simply supported)		
	TBSWI	BSWI	SHELL63	GangaRao	Morley	TBSWI	BSWI	SHELL63
	968DOFs	363DOFs	38400DOFs	/	/	968DOFs	363DOFs	38400DOFs
90°	4.0625	4.0625	4.0617	4.06	4.06	0..4788	0.4814	0.4786
85°	4.0140	4.0134	4.0150	4.01	4.01	0.4725	0.4770	0.4752
80°	3.8715	3.8683	3.8683	3.87	3.87	0.4556	0.4640	0.4637
75°	3.6429	3.6343	3.6362	3.64	-	0.4324	0.4427	0.4455
70°	3.3394	3.3228	3.3290	-	-	0.4058	0.4140	0.4210
60°	2.5712	2.5419	2.5581	2.56	2.56	0.3452	0.3374	0.3557
55°	2.1463	2.0929	2.1349	2.14	-	0.3109	0.2917	0.3170
50°	1.7230	1.6955	1.7144	1.72	1.72	0.2741	0.2429	0.2761
45°	1.3219	1.2830	1.3165	1.32	-	0.2355	0.1931	0.2340
40°	0.0961	0.9264	0.9584	0.958	0.958	1.9595	0.1445	0.1923
30°	0.4081	0.3883	0.4084	0.406	0.408	1.1924	0.0623	0.1145
'Exact' 30° (thin plate) 0.408							1.080	

Table 6 Central displacement and moment of a skew Reissner-Mindlin plate under distributed load

Skew angle α	$w1000D_0/qL^4$ (clamp supported)					$M10/qL^2$ (clamp supported)		
	TBSWI	BSWI	SHELL63	GangaRao	Morley	TBSWI	BSWI	SHELL63
	968DOFs	363DOFs	38400DOFs	/	/	968DOFs	363DOFs	38400DOFs
90°	1.2653	1.2652	1.2656	1.27	1.26	0.2290	0.2329	0.2287
85°	1.2488	1.2487	1.2499	-	-	0.2270	0.2306	0.2271
80°	1.2005	1.2002	1.2007	1.20	1.20	0.2213	0.2238	0.2211
75°	1.1232	1.1226	1.1232	-	-	0.2119	0.2129	0.2115
70°	1.0215	1.0206	1.0213	1.02	1.02	0.1992	0.1983	0.1988
60°	0.7694	0.7680	0.7692	0.771	0.769	0.1658	0.1609	0.1652
55°	0.6333	0.6317	0.6334	-	-	0.1464	0.1395	0.1456
50°	0.5002	0.4982	0.5005	0.503	0.500	0.1261	0.1173	0.1251
45°	0.3766	0.3741	0.3771	-	-	0.1056	0.0948	0.1043
40°	0.2678	0.2648	0.2684	0.269	0.270	0.0855	0.0728	0.0841
30°	0.1077	0.1039	0.1083	0.108	-	0.0490	0.0334	0.0477

value' in reference (Zienkiewicz 1988), we can see TBSWI also performs well in small angle problems, so it is suitable for singular problems.

Table 7 shows the vibration problems of a skew Reissner-Mindlin plate with different boundary conditions and skew angles. From comparison with reference (Liew *et al.* 1993), the two sets of their results are in good agreement with each other under different boundary condition and skew angle. Therefore, TBSWI element is an effective and stable way to the bending and vibration problems of square and skew Reissner-Mindlin plate, as well as suitable for singular problems.

Table 7 The first four natural frequencies of a skew Reissner-Mindlin plate (Frequency parameters $\Omega_i = \omega_i L^2(\rho t/D_0)^{1/2}(\mathrm{rad}\cdot\mathrm{s}^{-1})$) ($t/L = 0.2$)

Boundary conditions	Skew angle α	90°		75°		60°	
	Method	TBSWI	Liew	TBSWI	Liew	TBSWI	Liew
	DOFs	968	/	968	/	968	/
CCCC	Ω_1	2.7250	2.6807	2.8036	2.8058	3.0588	3.2313
	Ω_2	4.8038	4.6753	4.6729	4.6298	4.7551	4.9757
	Ω_3	4.8038	4.6761	5.1520	5.0963	5.7676	6.0140
	Ω_4	6.4781	6.2761	6.3944	6.3070	6.3520	6.6217
	Ω_5	7.4095	7.1496	7.5445	7.4052	7.9779	8.2634
SSSS	Ω_1	1.6969	1.7661	1.7537	1.8560	1.9469	2.1719
	Ω_2	3.8800	3.8580	3.7397	3.7856	3.8026	4.0637
	Ω_3	3.8800	3.8580	4.2366	4.2763	4.8837	5.1849
	Ω_4	5.5879	5.5737	5.5124	5.5784	5.4701	5.8321
	Ω_5	6.7616	6.5820	6.9044	6.8385	7.2910	7.7066
SCSC	Ω_1	2.3013	2.2606	2.3884	2.3682	2.6725	2.7383
	Ω_2	4.1358	4.0286	4.1706	4.1091	4.3546	4.4680
	Ω_3	4.6343	4.5063	4.8452	4.7862	5.4511	5.6513
	Ω_4	6.0934	5.9139	6.0070	5.9221	5.9945	6.2009
	Ω_5	6.8315	6.6445	7.1072	7.0138	7.6910	7.9691
CFFF	Ω_1	0.3408	0.3382	0.3446	0.3479	0.3537	0.3769
	Ω_2	0.7613	0.7437	0.7639	0.7588	0.7802	0.8161
	Ω_3	1.8518	1.7779	1.8800	1.8299	1.9441	1.9772
	Ω_4	2.4129	2.2741	2.2596	2.1886	2.1119	2.1627
	Ω_5	2.5283	2.4163	2.7401	2.6309	3.0911	3.0974
CFCF	Ω_1	1.7928	1.7732	1.8329	1.8438	1.9591	2.0781
	Ω_2	2.0651	2.0104	2.0818	2.0606	2.1428	2.2343
	Ω_3	3.3564	3.1590	3.3808	3.2396	3.4721	3.5201
	Ω_4	4.1352	4.0281	4.2134	4.1701	4.4231	4.5966
	Ω_5	4.4929	4.3336	4.5604	4.4612	4.7855	4.8934
SFSF	Ω_1	0.9218	0.9096	0.9981	0.9519	1.2218	1.0907
	Ω_2	1.4684	1.4267	1.4997	1.4467	1.6167	1.5163
	Ω_3	3.1325	2.9482	3.0982	2.9277	3.1104	2.9640
	Ω_4	3.2562	3.1630	3.3812	3.3090	3.7323	3.7388
	Ω_5	3.7861	3.6369	3.9390	3.8272	4.3408	4.3575

S: simply supported
C: clamp supported
F: free

4. The construction of TBSWI element for Reissner-Mindlin plate on an elastic foundation

4.1 TBSWI element formulation for the bending analysis of a Reissner-Mindlin plate on elastic foundation

Under homogeneous boundary conditions, the generalized potential energy function with two kinds of variables for bending problems for Reissner-Mindlin plate on an elastic foundation is (Shen 1997)

$$\Pi_{2p} = \int_{\Omega} \mathbf{M}^T \boldsymbol{\chi} dxdy + \int_{\Omega} \mathbf{Q}^T \boldsymbol{\gamma} dxdy - \int_{\Omega} \frac{1}{2} \mathbf{M}^T \mathbf{D}_b^{-1} \mathbf{M} dxdy - \int_{\Omega} \frac{1}{2} \mathbf{Q}^T C_b^{-1} \mathbf{Q} dxdy - \int_{\Omega} \Delta^T \mathbf{P} dxdy + \frac{1}{2} \int_{\Omega} k_e w^2 dxdy \tag{24}$$

where $k_e = \bar{k} D_b / L^4$ is the Winkler foundation coefficient, $\bar{k}$ is Winkler constant. Other symbols are the same as in Eq. (11).

Taking the scaling functions of two-dimensional tensor product BSWI in Eq. (5) as interpolating function, and translating the field variables into standard solving domain. According to the generalized variational principle $\delta\Pi_{2p}/\partial M_{\xi}^{e} = 0, \delta\Pi_{2p}/\partial M_{\eta}^{e} = 0, \delta\Pi_{2p}/\partial M_{\xi\eta}^{e} = 0, \delta\Pi_{2p}/\partial Q_{\xi}^{e} = 0$, $\delta\Pi_{2p}/\partial Q_{\eta}^{e} = 0$, $\delta\Pi_{2p}/\partial \theta_{\xi}^{e} = 0$, $\delta\Pi_{2p}/\partial \theta_{\eta}^{e} = 0$, and $\delta\Pi_{2p}/\partial w^{e} = 0$, the TBSWI element formulation for bending analysis of Reissner-Mindlin plate on an elastic foundation is

$$\begin{bmatrix} \mathbf{F} & \mathbf{H} \\ \mathbf{H}^T & \mathbf{S} \end{bmatrix} \begin{bmatrix} \mathbf{a} \\ \mathbf{b} \end{bmatrix} = \begin{bmatrix} 0 \\ \mathbf{P} \end{bmatrix} \tag{25}$$

where

$$\mathbf{F} = \begin{bmatrix} \frac{-12}{Et^3}\Gamma_1^{00}\otimes\Gamma_2^{00} & \frac{12\mu}{Et^3}\Gamma_1^{00}\otimes\Gamma_2^{00} & 0 & 0 & 0 \\ \frac{12\mu}{Et^3}\Gamma_1^{00}\otimes\Gamma_2^{00} & \frac{-12}{Et^3}\Gamma_1^{00}\otimes\Gamma_2^{00} & 0 & 0 & 0 \\ 0 & 0 & \frac{-24(1+\mu)}{Et^3}\Gamma_1^{00}\otimes\Gamma_2^{00} & 0 & 0 \\ 0 & 0 & 0 & \frac{-12(1+\mu)}{5Et}\Gamma_1^{00}\otimes\Gamma_2^{00} & 0 \\ 0 & 0 & 0 & 0 & \frac{-12(1+\mu)}{5Et}\Gamma_1^{00}\otimes\Gamma_2^{00} \end{bmatrix}$$

$$\mathbf{H} = \begin{bmatrix} 0 & -\Gamma_1^{01}\otimes\Gamma_2^{00} & 0 \\ 0 & 0 & -\Gamma_1^{00}\otimes\Gamma_2^{01} \\ 0 & -\Gamma_1^{00}\otimes\Gamma_2^{01} & -\Gamma_1^{01}\otimes\Gamma_2^{00} \\ -\Gamma_1^{01}\otimes\Gamma_2^{00} & \Gamma_1^{00}\otimes\Gamma_2^{00} & 0 \\ -\Gamma_1^{00}\otimes\Gamma_2^{01} & 0 & \Gamma_1^{00}\otimes\Gamma_2^{00} \end{bmatrix}$$

$$\mathbf{S} = \begin{bmatrix} k_e \Gamma_1^{00} \otimes \Gamma_2^{00} & 0 & 0 \\ 0 & 0 & 0 \\ 0 & 0 & 0 \end{bmatrix}$$

$$\mathbf{a} = [M_\xi^e \;\; M_\eta^e \;\; M_{\xi\eta}^e \;\; Q_\xi^e \;\; Q_\eta^e]^T$$

$$\mathbf{b} = [w \;\; \theta_\xi^e \;\; \theta_\eta^e]^T$$

To distributed load, $\mathbf{P} = [(\mathbf{T}^e)^T L_x L_y \sin\alpha \int_0^1 \int_0^1 q \boldsymbol{\phi}_1^T \otimes \boldsymbol{\phi}_2^T dxdy \;\; 0 \;\; 0]^T$. To concentrated load, $\mathbf{P} = [(\mathbf{T}^e)^T L_x L_y \sin\alpha \int_0^1 \int_0^1 q\,\delta(x-\xi)\delta(y-\eta)\boldsymbol{\phi}_1^T \otimes \boldsymbol{\phi}_2^T dxdy \;\; 0 \;\; 0]^T$, where ξ and η are the coordinates at the concentrated load point.

The integral terms are as follows

$$\Gamma_1^{00} = (\mathbf{T}^e)^T L_x \int_0^1 \boldsymbol{\Phi}_1^T \boldsymbol{\Phi}_1 d\xi (\mathbf{T}^e)$$

$$\Gamma_1^{10} = (\mathbf{T}^e)^T \int_0^1 \frac{d\boldsymbol{\Phi}_1^T}{d\xi} \boldsymbol{\Phi}_1 d\xi (\mathbf{T}^e)$$

$$\Gamma_1^{20} = (\mathbf{T}^e)^T \frac{1}{L_x} \int_0^1 \frac{d^2\boldsymbol{\Phi}_1^T}{d\xi^2} \boldsymbol{\Phi}_1 d\xi (\mathbf{T}^e)$$

$$\Gamma_1^{01} = (\Gamma_1^{10})^T$$

$$\Gamma_1^{02} = (\Gamma_1^{20})^T$$

We can obtain $\Gamma_1^{i,j}(i,j=0,1,2)$ by substituting L_x and $d\xi$ with L_y and $d\eta$ in $\Gamma_2^{i,j}(i,j=0,1,2)$.

4.2 Numerical examples

Numerical examples of the bending analysis of Reissner-Mindlin plates on an elastic foundation are provided here to verify the efficiency of the multivariable wavelet finite elements constructed in section 4.1. BSWI4_3 (the 4th order BSWI scaling functions at scale $j=3$) is chosen as the interpolating function.

The relative parameters of a Reissner-Mindlin plate on an elastic foundation in Fig. 5 are as follows: Length $L = L_x = L_y = 1$ m; Elastic modulus $E = 3\times10^4$ N/m^2; Thickness $t = 0.05$ m; Poisson ratio $\mu = 0.3$; Density $\overline{m} = 7917$ kg/m^3; Uniform load $q = -1$ N/m^2.

Table 8 provides the analysis of the bending problem of Reissner-Mindlin plates on an elastic foundation with four different boundary conditions. Fig. 6 shows the corresponding deformation maps with Winlker constant $\overline{k} = 5$, which is in consistent with the practical deformation. In detail, comparison with SHELL63 (38400DOFs) reveals that TBSWI (968DOFs) performs well in bending analysis of Reissner-Mindlin plate on elastic foundation. With much smaller DOFs, only 2.6% of

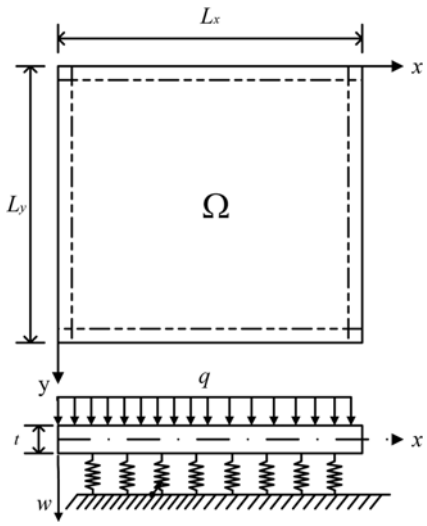

Fig. 5 The solving domain and relative parameters of a Reissner-Mindlin plate on an elastic foundation

Table 8 Central displacement and moment of a Reissner-Mindlin plate on an elastic foundation with distributed load under different boundary conditions

Boundary condition	Winkler constant	Methods	$100w$	$10M_x$	$10M_y$
SSSS	$\bar{k}=5$	TBSWI (968DOFs)	1.18252	0.47202	0.47202
		SHELL63 (38400DOFs)	1.16750	0.47185	0.47185
	$\bar{k}=100$	TWFEM (968DOFs)	0.94489	0.36931	0.36931
		SHELL63 (38400DOFs)	0.93570	0.37031	0.37031
CCCC	$\bar{k}=5$	TBSWI (968DOFs)	0.38484	0.22924	0.22924
		SHELL63 (38400DOFs)	0.36706	0.22781	0.22781
	$\bar{k}=100$	TWFEM (968DOFs)	0.35599	0.20975	0.20975
		SHELL63 (38400DOFs)	0.34090	0.20938	0.20938
SFSF	$\bar{k}=5$	TBSWI (968DOFs)	3.64856	1.15914	0.24333
		SHELL63 (38400DOFs)	3.31730	1.16090	0.25702
	$\bar{k}=100$	TWFEM (968DOFs)	1.83941	0.56973	0.12471
		SHELL63 (38400DOFs)	1.83390	0.57366	0.13123
CSSS	$\bar{k}=5$	TBSWI (968DOFs)	0.82370	0.38833	0.33806
		SHELL63 (38400DOFs)	0.80373	0.38486	0.33325
	$\bar{k}=100$	TWFEM (968DOFs)	0.69917	0.32466	0.28151
		SHELL63 (38400DOFs)	0.68490	0.32326	0.27869

S: simply supported
C: clamp supported
F: free

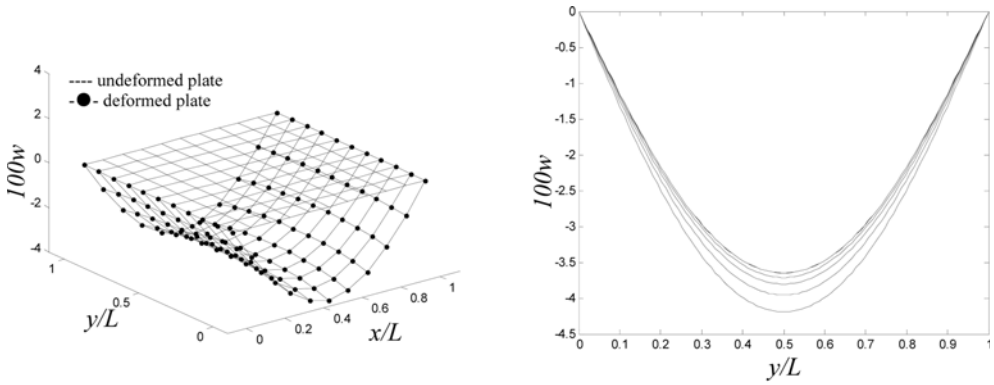

(a) Deformation of the square plate (zoomed 100 times) (b) Isoline along x

Fig. 6 Deformation map of a Reissner-Mindlin plate on an elastic foundation simply supported on two opposite sides and the other free, with $\bar{k} = 5$

SHELL63 element, TBSWI obtains results in same accuracy of SHELL63. Besides, it is noteworthy that TBSWI has done very well in moment calculation. It obtains the results of displacement and moment in similar accuracy because they are separately interpolated. Therefore, TBSWI is an effective way with high efficiency and high precision, which can do good job both in displacement and moment calculation.

5. Conclusions

A new multivariable finite element with two kinds of variables based on BSWI is constructed in this study. The multivariable BSWI elements of a square Reissner-Mindlin plate, a skew Reissner-Mindlin plate, and a Reissner-Mindlin plate on an elastic foundation are studied. The finite element formulations are developed from a generalized potential energy functional based on a generalized variational principle, and BSWI is treated as trial function in this method. As compared to the conventional method, the elements proposed in this study can apparently improve calculation accuracy. Moment can be directly calculated by solving the finite element formulations because they are treated as independent variables while in the traditional method, they are calculated by differentiation of displacement, thus introducing calculation error and affecting accuracy. Another superiority of the elements constructed is the interpolating function. Unlike the commonly used Daubechies wavelet, BSWI has explicit expression, which makes integration and differentiation conveniently. Besides, the good approximation property of BSWI further guarantees the accuracy of final results.

Several numerical examples of bending and vibration analysis of a square Reissner-Mindlin plate, a skew Reissner-Mindlin plate, and a Reissner-Mindlin plate on an elastic foundation are studied. The examples provide results and validate the effectiveness of these elements. Therefore, it can be concluded that the method proposed in this study is an effective and efficient way for static and vibration problems of Reissner-Mindlin plate.

Acknowledgements

This work is supported by the National Natural Science Foundation of China (No. 50875195), the Foundation for the Author of National Excellent Doctoral Dissertation of China (No. 2007B33), and the key project of the National Natural Science Foundation of China (No. 51035007).

References

Basu, P.K., Jorge, A.B. and Badri, S. (2003), "Higher-order modeling of continua by finite-element, boundary-element, Meshless, and wavelet methods", *Comput. Math. Appl.*, **46**, 15-33.

Bathe, K.J., Bucalem, M. and Brezzi, F. (1990), "Displacement and stress convergence of our MITC plate bending elements", *Eng. Comput.*, **7**(4), 291-302.

Brezzi, F., Bathe, K.J. and Fortin, M. (1989), "Mixed-Interpolated elements for Reissner-Mindlin plates", *Int. J. Numer. Meth. Eng.*, **28**, 1787-1801.

Canuto, C., Tabacco, A. and Urban, K. (1996), "The wavelet element method Part I: Construction and analysis", *Appl. Comput. Harmon. Analy.*, **6**, 1-52.

Canuto, C., Tabacco, A. and Urban, K. (2000), "The wavelet element method Part II: Realization and Additional Feature in 2D and 3D", *Appl. Comput. Harmon. Analy.*, **8**, 123-165.

Chen, W.H. and Wu, C.W. (1996), "Extension of spline wavelets element method to membrane vibration analysis", *Comput. Mech.*, **18**(1), 46-54.

Chen, X.F., Yang, S.J. and He, Z.J. (2004), "The construction of wavelet finite element and its application", *Finite Elem. Analys. Des.*, **40**, 541-554.

Chui, C.K. and Ewald, Q. (1992), "Wavelets on a bounded interval", *Numer. Meth. Approx. Theory*, **1**, 53-57.

Cohen, A. (2003), *Numerical Analysis of Wavelet Method*, Elsevier Press, Amsterdam, Holland.

Diaz, L.A., Martin, M.T. and Vampa, V. (2009), "Daubechies wavelet beam and plate finite elements", *Finite Elem. Analys. Des.*, **45**(3), 200-209.

Goswami, J.C., Chan, A.K. and Chui, C.K. (1995), "On solving first-kind integral equations using wavelets on a bounded interval", *IEEE T. Antenn. Propag.,* **43**, 614-622.

Han, J.G., Ren, W.X. and Huang, Y. (2005), "A multivariable wavelet-based finite element method and its application to thick plates", *Finite Elem. Analys. Des.*, **41**, 821-833.

He, Y.M. and Chen, X.F. (2008), "Multiresolution analysis for finite element method using interpolating wavelet and lifting scheme", *Commun. Numer. Meth. Eng.*, **24**(11), 1045-1066.

Hellinger, E. (1914), "Der Allgemeine Ansatz der Mechanik der Kontinua", Encyclopadia der Matematischen Wissenschaften, 4.

Hu, B., Wang, Z. and Xu, Y.C. (2010), "Combined hybrid method applied in the Reissner-Mindlin plate model", *Finite Elem. Analy. Des.*, **46**(5), 428-437.

Hu, H.C. (1954), "On some variational principles in the theory of elasticity and the theory of plasticity", *Acta Physica Sinica*, **10**(3), 259-289.

Hu, H.C. (1981), *The Variational Principle of Elastic Mechanics and Its Application*, Science Press, Beijing.

Lee, P.S. and Bathe, K.J. (2010), "The quadratic MITC plate and MITC shell elements in plate bending", *Adv. Eng. Software,* **41**, 712-728.

Liew, K.M., Xiang, Y., Kittipornchai, S. and Wang, C.M. (1993), "Vibration of thick skew plates based on Mindlin shear deformation plate theory", *J. Sound Vib.*, **168**(1), 39-69.

Liu, Y. and Soh, C.K. (2007), "Shear correction for Mindlin type plate and shell elements", *Int. J. Numer. Meth. Eng.,* **69**(13), 2789-2806.

Liu, Y., Hu, N., Yan, C., Peng, X. and Yan, B. (2009), "Construction of a Mindlin pseudospectral plate element and evaluating efficiency of the element", *Finite Elem. Analys. Des.*, **45**(8-9), 538-546.

Long, Y.Q. and Xi, F. (1992), "A universal method for including shear deformation in thin plate elements", *Int. J. Numer. Meth. Eng.*, **34**, 171-177.

Long, Y.Q., Long, Z.F. *et al.* (2004), *A New Theory of Finite Element Method*, Tsinghua University Press,

Beijing.
Morley, L.S.D. (1963), *Skew Plates and Structures,* Pergamon Press, New York.
Petersen, S., Farhat, C. and Tezaur, R. (2009), "A space-time discontinuous Galerkin method for the solution of the wave equation in the time domain", *Int. J. Numer. Meth. Eng.*, **78**, 275-295.
Quak, E. and Weyrich, N. (1994), "Decomposition and reconstruction algorithms for spline wavelets on a bounded interval", *Appl. Comput. Harmon. Analy.*, **1**(3), 217-231.
Rao, H.V.S.G. and Chaudhary, V.K. (1998), "Analysis of skew and triangular plates in bending", *Comput. Struct.*, **28**(2), 223-235.
Reissner, E. (1950), "On a variational theorem in elasticity", *J. Math. Phys.*, **29**, 90-95.
Shen, P.C. (1991), *Spline Finite Methods in Structural Analysis*, Hydraulic and Electric Press, Beijing.
Shen, P.C. (1997), *Multivariable Spline Finite Element Method*, Science Press, Beijing.
Shen, P.C. and He, P.X. (1995), "Bending analysis of rectangular moderately thick plates using spline finite-element method", *Int. J. Solids Struct.*, **54**(6), 1023-1029.
Shen, P.C., He, P.X. and Su, G.L. (1992), "Stability analysis for plates using the multivariable spline element method", *Comput. Struct.*, **45**(5-6), 1073-1077.
Wang, Y.M., Chen, X.F., He, Y.M. and He, Z.J. (2010), "New decoupled wavelet bases for multiresolution structural analysis", *Struct. Eng. Mech.*, **35**(2), 175-190.
Warburton, G.B. (1954), "The vibration of rectangular plates", *Proceed. Institut. Mech. Eng.*, **168**, 371-385.
Washizu, K. (1955), "On the variational principles of elasticity and plasticity", Aeroelasticity and Structures Research Laboratory, Massachusetts Institute of Technology, Technical Report, 25-18.
Xiang, J.W. and Chen, X.F. (2006), "The construction of plane elastomechanics and Mindlin plate elements of B-spline wavelet on the interval", *Finite Elem. Analy. Des.*, **42**, 1269-1280.
Xiang, J.W., Chen, X. and He, Z. (2007), "Static and vibration analysis of thin plates by using finite element method of B-spline wavelet on the interval", *Struct. Eng. Mech.*, **25**(5), 613-629.
Xiang, Y., Lai, S.K. and Zhou, L. (2010), "DSC-element method for free vibration analysis of rectangular Mindlin plates", *Int. J. Mech. Sci.*, **52**(4), 548-560.
Zhang, X.W., Chen, X.F., Wang, X.Z. and He, Z.J. (2010), "Multivariable finite elements based on B-spline wavelet on the interval for thin plate static and vibration analysis", *Finite Elem. Analys. Des.*, **46**(5), 416-427.
Zienkiewicz, D.L. (1988), "A robust triangular plate bending element of the Reissener-Mindlin type", *Int. J. Numer. Meth. Eng.*, **26**, 1169-1184.
Zienkiewicz, O.C., Taylor, R.L. and Zhu, J.Z. (2005), *The Finite Element Method,* Heinemann, Butterworth.